

Defective Angiogenesis in Mice Lacking Endoglin

Dean Y. Li,^{1,3,4*} Lise K. Sorensen,⁵ Benjamin S. Brooke,^{1,3,4}
 Lisa D. Urness,⁵ Elaine C. Davis,⁶ Douglas G. Taylor,^{1,2}
 Beth B. Boak,⁵ Daniel P. Wendel^{1,2}

Endoglin is a transforming growth factor- β (TGF- β) binding protein expressed on the surface of endothelial cells. Loss-of-function mutations in the human endoglin gene *ENG* cause hereditary hemorrhagic telangiectasia (HHT1), a disease characterized by vascular malformations. Here it is shown that by gestational day 11.5, mice lacking endoglin die from defective vascular development. However, in contrast to mice lacking TGF- β , vasculogenesis was unaffected. Loss of endoglin caused poor vascular smooth muscle development and arrested endothelial remodeling. These results demonstrate that endoglin is essential for angiogenesis and suggest a pathogenic mechanism for HHT1.

HHT is an autosomal dominant vascular dysplasia characterized by recurrent epistaxis, telangiectasia, gastrointestinal hemorrhage, and pulmonary, cerebral, and hepatic arteriovenous malformations (1). *ENG*, the gene responsible for HHT1, encodes an endothelial transmembrane protein that binds to members of the TGF- β superfamily and their receptor complexes (2, 3). TGF- β signaling is required for the first stage of vascular development, vasculogenesis, when the primary capillary network, composed of interconnected and homogeneously sized endothelial tubes, is formed (4). The second stage of vascular development, angiogenesis, involves remodeling the primary endothelial network into a mature circulatory system (5, 6). To understand the role of endoglin in vascular development, we used gene targeting to generate mice lacking endoglin.

The targeting vector was designed to replace the first two exons with a gene that conferred neomycin resistance (7) (Fig. 1A). Three targeted embryonic stem (ES) cell clones were identified and used to generate chimeric mice by morula aggregation. Southern blot analysis confirmed germ line transmission of the targeted allele (Fig. 1B). Immunohistochemistry was used to detect endoglin in the endothelium of *Eng*^{+/+} and *Eng*^{+/-} mice by embryonic day 8.5 (E8.5), but neither endoglin protein nor mRNA was detected in *Eng*^{-/-} mice (8) (Fig. 1, C to E). The life expectancy, fertility, and gross appearance of *Eng*^{+/-} F₁ and F₂ mice were

normal; however, no homozygotes were found among 150 newborn animals from heterozygous intercrosses. By examining embryos from heterozygous intercrosses at different developmental stages, we determined that no *Eng*^{-/-} mice survive after E11.5.

At E10.5, *Eng*^{-/-} mice were three times smaller than *Eng*^{+/+} mice and had fewer somites (18 to 22 in *Eng*^{-/-} mice and 32 to 35 in *Eng*^{+/+} mice). These *Eng*^{-/-} embryos exhibited an absence of vascular organization and the presence of multiple pockets of red blood cells on the surface of the yolk sac (Fig. 1, F and G). Expression of endothelial markers such as Flk-1, Flt-1, Tie-1, and Tie-2 and hematopoietic markers Gata-1 and Il-3r were not disrupted in *Eng*^{-/-} mice (9). Thus, in contrast to TGF- β 1 or its signaling receptor, there is no evidence that endoglin is required for endothelial differentiation or primitive hematopoiesis (4). The absence of organized vessels in the *Eng*^{-/-} yolk sacs was confirmed by immunohistochemical staining for the endothelial marker platelet-endothelial cell adhesion molecule (PECAM) (Fig. 1, H and I) (10). The persistence of an immature perineural vascular plexus indicated a failure of endothelial remodeling in *Eng*^{-/-} embryos (Fig. 1, J and K). At E10.5, the cardiac tube did not complete rotation in *Eng*^{-/-} mice and was associated with a serosanguinous pericardial effusion (11). Although the cardiac tube continued to circulate blood at E10.5, by E11.5 there was evidence of resorption and necrosis in *Eng*^{-/-} embryos.

PECAM immunostains demonstrated that the first organ system affected in *Eng*^{-/-} embryos was the vascular system. At E8.5 and E9.5, the endothelial organization of *Eng*^{+/+} and *Eng*^{-/-} embryos was similar (Fig. 2, A, B, E, and F). However, between E9.5 and E10.5, vascular development was disrupted in *Eng*^{-/-} mice. Although there was extensive endothelial remodeling of the vasculature with expansion of existing vessels and sprouting and branching of new ones in

Eng^{+/+} embryos at E10.5, the major vessels including the dorsal aortae, intersomitic vessels, branchial arches, and carotid arteries were atretic and disorganized in *Eng*^{-/-} embryos (Fig. 1, J and K, and Fig. 2, I and J).

Because TGF- β signaling has been shown to regulate vascular smooth muscle cell (vsmc) differentiation in vitro, we hypothesized that the disrupted angiogenesis in *Eng*^{-/-} embryos was due to poor vsmc development (6). We stained embryos with an antibody to alpha smooth muscle cell actin (α -smc actin) to assess vsmc development. At E8.5 (10- to 12-somite stage), *Eng*^{+/+} and *Eng*^{-/-} embryos were indistinguishable, with a foci of vsmc forming at the cranial-most aspect of the dorsal aortae (Fig. 2, C and D). By E9.5 (18- to 20-somite stage), *Eng*^{+/+} vsmc had extended rostrally to the carotid arteries and caudally through the dorsal aortae (Fig. 2G). At E10.5, vsmc of the *Eng*^{+/+} embryos surrounded the dorsal aortae, branchial arches, and carotid arteries (Fig. 2K). In contrast, there was poor vsmc formation of *Eng*^{-/-} embryos at both E9.5 and E10.5 (Fig. 2, H and L). Thus, significant differences in development of *Eng*^{+/+} and *Eng*^{-/-} vsmc were apparent by E9.5 and preceded the differences in endothelial organization observed between E9.5 and E10.5.

The failure in endothelial remodeling was not restricted to embryonic tissue. Vascular organization of E8.5 *Eng*^{+/+} and *Eng*^{-/-} yolk sacs was similar and consisted of a primary endothelial network (Fig. 3, A and B). At E9.5, distinct vessels were forming in *Eng*^{+/+} yolk sac (Fig. 3E). In contrast, the vasculature of E9.5 *Eng*^{-/-} yolk sacs failed to organize (Fig. 3F). By E10.5, distinct vessels were prominent in *Eng*^{+/+} mice but absent in *Eng*^{-/-} mice (Fig. 1, H and I). Although disruption of endothelial organization occurs between E9.5 and E10.5, poor vsmc development is evident by E8.5 in *Eng*^{-/-} yolk sacs. At E8.5, vsmc coated selective endothelial tubes in the *Eng*^{+/+} yolk sac but were scarce in the *Eng*^{-/-} yolk sac (Fig. 3, C and D). By E9.5, vsmc in *Eng*^{+/+} yolk sacs outlined distinct vessels, whereas no progression was seen in *Eng*^{-/-} yolk sacs (Fig. 3, G and H). Thus, the vsmc defect in *Eng*^{-/-} extraembryonic tissue was evident by E8.5 and preceded the defect in endothelial remodeling.

We used histologic analysis, in situ hybridization, and ultrastructural analysis to confirm that vascular development is disrupted in *Eng*^{-/-} mice. Cross sections of α -smc actin immunostains identified vsmc between the endoderm and endothelium of the yolk sac. Few vsmc formed between these layers in *Eng*^{-/-} compared with *Eng*^{+/+} yolk sacs (Fig. 4, A and B). Transverse sections of dorsal aortae showed vsmc developing around the endothelium of an *Eng*^{+/+} em-

¹Program in Human Molecular Biology and Genetics, ²Department of Human Genetics, ³Department of Oncological Sciences, ⁴Department of Medicine, ⁵Howard Hughes Medical Institute, University of Utah, Salt Lake City, UT 84112-5330, USA, ⁶Department of Cell Biology and Neuroscience, University of Texas, Southwestern Medical Center, Dallas, TX 75235-9039, USA.

*To whom correspondence should be addressed. E-mail: dean.li@hci.utah.edu

REPORTS

bryo at E9.5 (Fig. 4C). No vsmc are observed in a comparable section of an *Eng*^{-/-} embryo (Fig. 4D). In situ hybridization for an

early molecular marker of vsmc development, SM22 α , showed a failure of vsmc to develop in E9.5 *Eng*^{-/-} yolk sac and em-

bryos (12) (Fig. 4, E, F, G, and H). Electron micrographs of E9.5 *Eng*^{-/-} yolk sacs illustrated the absence of supporting cells, pre-

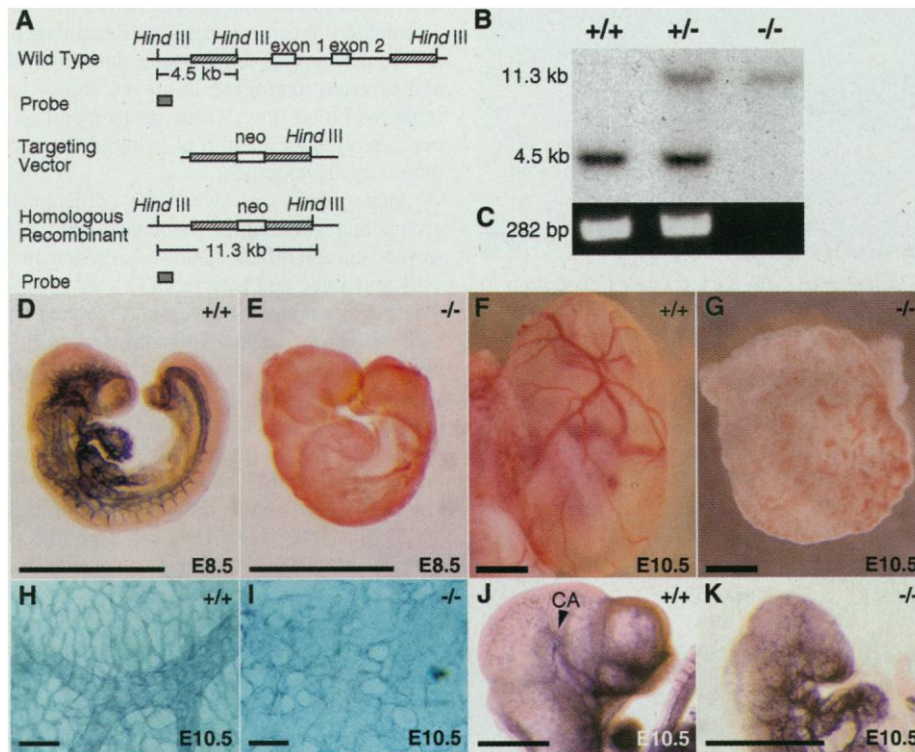


Fig. 1. Targeted inactivation of murine *Eng* results in defective vascular development. (A) Restriction maps of *Eng* genomic fragment, targeting construct, and predicted structure of targeted *Eng* allele. Hatched boxes represent regions of homology shared by the targeting vector and genomic *Eng*. The probe for Southern blot analysis detects an 11.3-kb Hind III fragment from the disrupted allele and a 4.5-kb Hind III fragment from the wild-type allele. (B) Southern blot analysis of yolk sac DNA from E10.5 embryos probed for homologous recombination. (C) Absence of *Eng* transcript in E9.5 *Eng*^{-/-} mice. Primers amplifying a 282-base pair region of *Eng* were used to amplify cDNA from total RNA. (D and E) Endoglin immunostain of E8.5 embryos demonstrates the presence and absence, respectively, of endoglin in *Eng*^{+/+} and *Eng*^{-/-} mice. (F and G) Photomicrographs of E10.5 yolk sacs. The vasculature of the *Eng*^{+/+} yolk sac is well defined. Pockets of red blood cells are observed in the *Eng*^{-/-} yolk sac with no discernible vessels. (H and I) PECAM immunostain of yolk sacs at E10.5. *Eng*^{-/-} endothelium fails to organize into vitelline vessels. (J and K) PECAM immunostain of head vessels at E10.5. The perineural capillary plexus fails to organize and the carotid artery (CA) is atretic in *Eng*^{-/-} embryos. (D to G, J, and K) Bar = 1.0 mm; (H and I) bar = 0.1 mm.

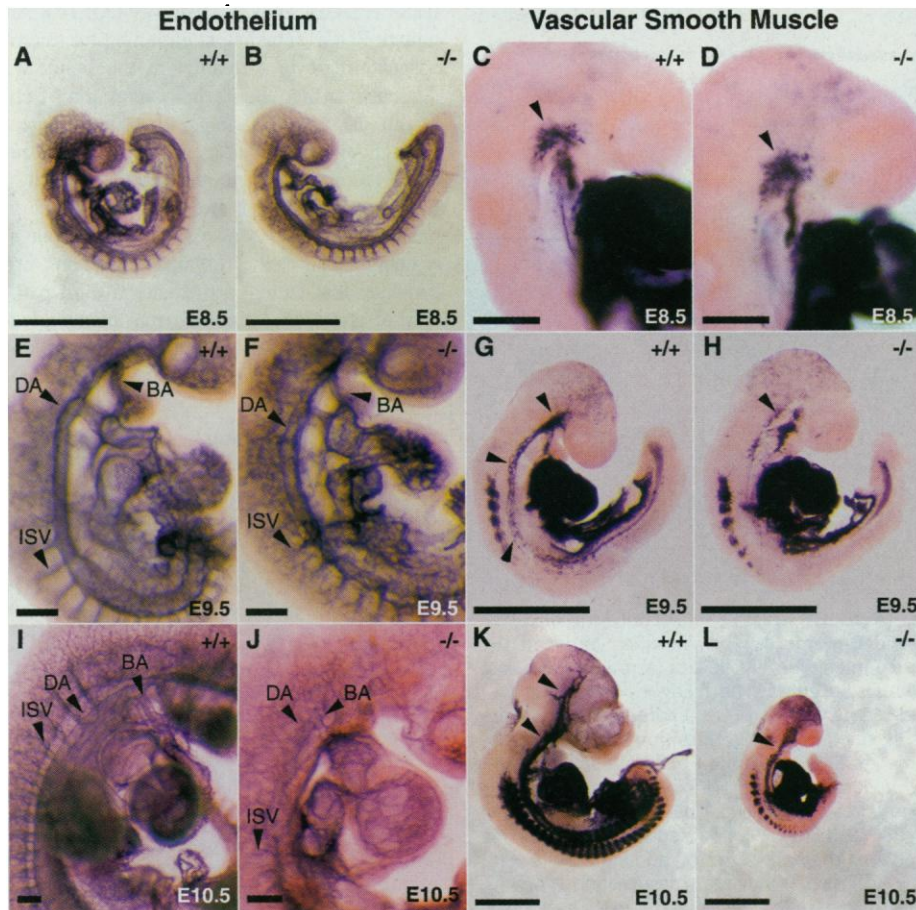


Fig. 2. Poor vascular smooth muscle development in *Eng*^{-/-} embryos precedes disruption in endothelial remodeling. Immunohistochemistry with antisera to PECAM (A, B, E, F, I, and J) and α -smc actin (C, D, G, H, K, and L). (A and B) At E8.5 the organization of *Eng*^{+/+} and *Eng*^{-/-} endothelial tubes is indistinguishable. (C and D) At E8.5, initiation of vsmc differentiation occurs at the cranial-most aspect of the dorsal aortae (arrowheads). (E and F) At E9.5 the endothelial organization of *Eng*^{+/+} and *Eng*^{-/-} embryos remains similar. The dorsal aorta (DA), branchial arches (BA), and intersomitic vessels (ISV) are identified. (G and H) vsmc formation in the *Eng*^{+/+} embryos extends caudally in the dorsal aortae and rostrally to the carotid arteries (arrowheads). vsmc development in *Eng*^{-/-} embryos fails to progress from E8.5 to E9.5. (I and J) There is a marked maturation of endothelial organization in *Eng*^{+/+} embryos that is lacking in *Eng*^{-/-} embryos. Large arteries like the carotid arteries, dorsal aortae, and intersomitic vessels are atretic in *Eng*^{-/-} embryos. (K and L) vsmc surround the carotid arteries and the dorsal aortae in *Eng*^{+/+} embryos (arrowheads). In comparison, vsmc formation in *Eng*^{-/-} embryos remains incomplete and sparse. (A, B, C, G, H, K, and L) Bar = 1.0 mm; (C, D, E, F, I, and J) bar = 0.2 mm.

REPORTS

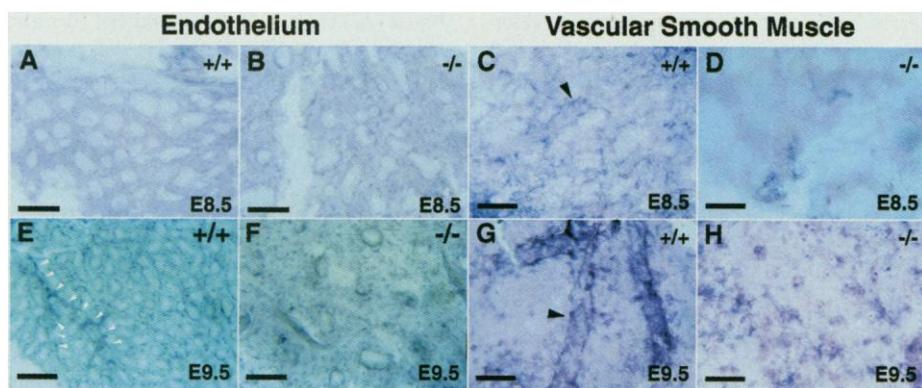


Fig. 3. Poor vascular smooth muscle development in *Eng*^{-/-} yolk sacs precedes disruption in endothelial remodeling. Immunohistochemistry using antisera to endothelial markers Flk-1 (A and B) and PECAM (E and F) and the vsmc marker α -smc actin (C, D, G, and H). (A and B) At E8.5, a primary endothelial network is present in both *Eng*^{+/+} and *Eng*^{-/-} yolk sacs. (C and D) At E8.5 vsmc (arrowhead) develop around selective endothelial tubes from *Eng*^{+/+} yolk sacs. vsmc formation is scarce and unorganized in *Eng*^{-/-} yolk sacs. (E and F) At E9.5, the primary endothelial network remodels into distinct vessels in *Eng*^{+/+} yolk sacs (arrowheads). There is no evidence of endothelial remodeling in E9.5 *Eng*^{-/-} yolk sacs. (G and H) At E9.5, vsmc define distinct vessels in *Eng*^{+/+} yolk sac but not in *Eng*^{-/-} yolk sac (arrowhead). Bar = 0.1 mm.

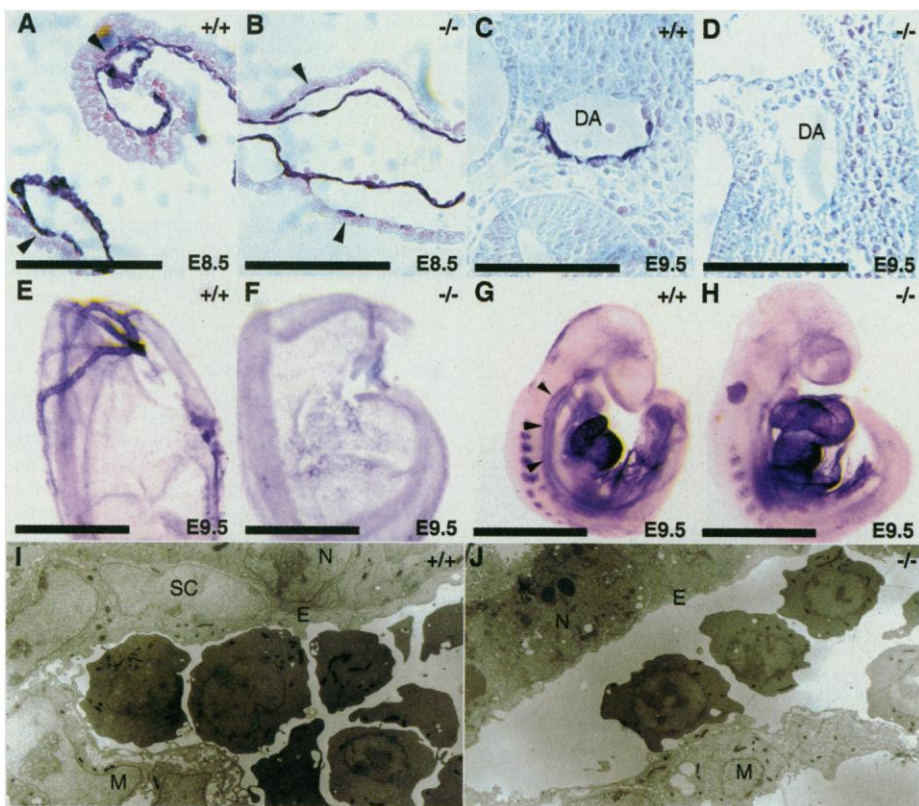


Fig. 4. Poor vsmc formation in *Eng*^{-/-} mice. (A to D) Transverse sections of anti-smc actin-stained embryos and yolk sacs at E9.5. (A and B) vsmc can be identified between the endoderm and endothelium in *Eng*^{+/+} and are scarce in *Eng*^{-/-} yolk sacs (arrowheads). Cross reactivity of α -smc actin antisera with the mesothelium is observed in both *Eng*^{+/+} and *Eng*^{-/-} yolk sacs. (C and D) vsmc form around the dorsal aortae (DA) of *Eng*^{+/+} embryos. No vsmc are identified in the dorsal aortae of *Eng*^{-/-} embryos. (E to H) In situ hybridization of yolk sacs and embryos at E9.5 using an RNA probe for the vsmc marker SM22 α . (E and F) Expression of SM22 α outlines *Eng*^{+/+} vessels and is absent in *Eng*^{-/-} yolk sacs. (G and H) Expression of SM22 α is present throughout the dorsal aortae of *Eng*^{+/+} embryos (arrowheads) but is absent from *Eng*^{-/-} embryos. (I and J) Electron micrographs of *Eng*^{+/+} and *Eng*^{-/-} yolk sac at E9.5. Supporting cells (SC), presumably vsmc or pericytes, are seen between the endoderm (N) and endothelium (E) of *Eng*^{+/+} yolk sacs but are absent in the *Eng*^{-/-} yolk sac. M indicates mesothelium. (A, B, C, and D) Bar = 0.1 mm; (E, F, G, and H) bar = 1.0 mm.

sumably pericytes or vsmc precursors, around the endothelium of the capillary network (13) (Fig. 4, I and J). Because vascular defects in *Eng*^{-/-} mice are observed before embryonic circulation is established and before defects in cardiogenesis are documented, it is unlikely that failed vsmc development and arrested angiogenesis are secondary to impaired blood flow. These data support our conclusion that endoglin is required for normal vsmc development.

Angiogenesis involves the differential growth and sprouting of endothelial tubes and recruitment and differentiation of mesenchymal cells into vsmc and pericytes (5). Our experiments demonstrate that endoglin is required for both processes. Because endoglin binds members of the TGF- β superfamily and interacts with their receptors, it is likely that endoglin regulates TGF- β signaling. This conclusion is supported by in vitro heterotypic coculture experiments in which endothelial cells induced vascular smooth muscle differentiation through a TGF- β pathway (14). Thus, our experiments indicate that TGF- β signaling is essential for angiogenesis.

Communication between the endothelium and mesenchyme is important for angiogenesis (5). Mesenchymal cells signal endothelial cells via the angiopoietin/Tie-2 signaling pathway, whereas endothelial cells induce differentiation of pericytes through the platelet-derived growth factor (PDGF) signaling pathway (15, 16). Although PDGF signaling is important for microvascular pericyte formation in the brain, we demonstrate that endothelial expression of endoglin is essential for vsmc development throughout the circulatory system. The subsequent failure of the endothelium to remodel in *Eng*^{-/-} mice after arrested vsmc development suggests that vsmc may also play a role in regulating endothelial organization. Thus, we conclude that endoglin mediates a third pathway of endothelial-mesenchymal communication that is essential for angiogenesis and important to the pathogenesis of vascular disease.

References and Notes

1. K. A. McAllister *et al.*, *Nature Genet.* **8**, 345 (1994); A. E. Guttmacher, D. A. Marchuk, R. I. White, *N. Engl. J. Med.* **33**, 918 (1995).
2. S. St-Jacques, U. Cymerman, N. Pece, M. Letarte, *Endocrinology* **134**, 2645 (1994); J. R. Westphal, H. W. Willems, C. J. M. Schalkwijk, D. J. Ruiter, R. M. W. De Waal, *J. Invest. Dermatol.* **100**, 27 (1993).
3. H. Yamashita *et al.*, *J. Biol. Chem.* **269**, 1995 (1994); S. Cheifetz *et al.*, *ibid.* **267**, 19027 (1992); N. P. Barbara, J. L. Wrana, M. Letarte, *ibid.* **274**, 584 (1999).
4. M. C. Dickson *et al.*, *Development* **121**, 1845 (1995); M. Oshima, H. Oshima, M. Taketo, *Dev. Biol.* **179**, 297 (1996).
5. J. Folkman and P. A. DiAmore, *Cell* **87**, 1153 (1996); G. D. Yancopoulos, M. Klagsbrun, J. Folkman, *ibid.* **93**, 661 (1998); I. Flamme and W. Risau, *Development* **116**, 435 (1992).
6. M. S. Pepper, *Cytokine Growth Factor Rev.* **8**, 21 (1993); D. M. Kingsley, *Genes Dev.* **8**, 133 (1994); A. H. Reddi, *Cytokine Growth Factor Rev.* **8**, 11 (1997); J. Massague, L. Allisano, J. L. Wrana, *Trends Cell Biol.* **4**, 172 (1994).

7. To construct a targeting vector, we used 3.5- and 5.2-kb fragments from a murine genomic ES BAC clone for the 5' and 3' regions of homology, respectively. Culture, selection, and screening of targeted clones were as described [D. Y. Li *et al.*, *Nature* **393**, 276 (1998)]. There was no evidence of random integration in the homologous recombinant clones used for chimera generation. Resulting chimeric animals were crossed to C57BL/6J mice and germ line transmission was confirmed. Genotypes were assigned on the basis of Southern blot analysis of DNA extracted from tails, embryos, or yolk sacs.
8. L. Sorensen and D. Li, unpublished data.
9. D. Wendel and D. Li, unpublished data. Reverse transcriptase-polymerase chain reactions for these molecular markers were done as described [F. Shalaby *et al.*, *Nature* **376**, 62 (1995)].
10. Immunoperoxidase staining of mouse embryos was done with monoclonal antibodies to PECAM (Pharmingen, San Diego, CA), endoglin (Pharmingen), FLK-1 (Santa Cruz Biotechnology, Santa Cruz, CA), or α -smc actin (clone 1A4, 1:500; Sigma, St. Louis, MO). Staining was developed in 3,3'-diaminobenzidine chromagen (Vector Laboratories, Burlingame, CA). Sections of stained tissue were counterstained with eosin B.
11. L. Sorensen, L. Urness, D. Li, unpublished data.
12. Hybridization was performed at 70°C with an RNA probe described by Li *et al.* [L. Li, J. M. Miano, P. Cserjesi, E. N. Olson, *Circulation* **78**, 188 (1996)]. Sense RNA probes showed no hybridization.
13. Tissue was fixed in 3% glutaraldehyde and sequentially stained with osmium tetroxide, tannic acid, and uranyl acetate. After dehydration, tissue was embedded in Epon. Thin sections (60 nm) were counterstained with uranyl acetate and lead citrate and examined on a JEOL 1200 electron microscope.

14. K. K. Hirschi, S. A. Rohovsky, P. A. DiAmore, *J. Cell. Biol.* **141**, 805 (1998).
15. C. Suri *et al.*, *Cell* **87**, 1171 (1996); T. Sato *et al.*, *Nature* **376**, 7074 (1995); P. C. Maisonnier *et al.*, *Science* **277**, 55 (1997).
16. P. Lindahl, B. R. Johansson, P. Levéon, C. Betsholtz, *Science* **277**, 242 (1997); P. Soriano, *Genes Dev.* **8**, 1888 (1994).
17. Supported by National Institutes of Health grants K08 HL03490-03 and T35 HL07744-06, the Culpeper Scholarship in Medical Science, and a University of Utah Seed Grant. We thank M. T. Keating for guidance and support and J. Miano and K. Thomas for clones and discussion. B.S.B. is a Howard Hughes Medical Institute Medical Student Research Training Fellow.

8 January 1999; accepted 13 April 1999

Equivalence in Yield from Marine Reserves and Traditional Fisheries Management

Alan Hastings^{1*} and Louis W. Botsford²

Marine reserves have been proposed as a remedy for overfishing and declining marine biodiversity, but concern that reserves would inherently reduce yields has impeded their implementation. It was found that management of fisheries through reserves and management through effort control produce identical yields under a reasonable set of simplifying assumptions corresponding to a broad range of biological conditions. Indeed, for populations with sedentary adults (invertebrates and reef fishes), reserves have important advantages for sustainability, making marine reserves the preferred management approach.

Marine reserves have been recommended as an alternative to existing fisheries management and as a means of conserving declining biodiversity. Where fisheries are concerned, reserves have been proposed to provide greater fishery yields when effort is high (1, 2), to prevent overfishing in the presence of parameter uncertainty (3), and to reduce variability in catch (2). However, the implementation of reserves has been slowed by concerns that they would reduce fishery yields substantially. In our study, we examined whether reserves can produce a yield equivalent to harvesting a fixed fraction or a fixed number of the population and determined a simple formula for the optimal fraction of area in reserves.

To assess this complex multifaceted problem, we made a number of simplifying, but robust, assumptions (4) that allowed us to focus on the essential issues. The most important assumptions are that adults are stationary, that larvae are distributed so broadly that the density of settling juveniles along the coastline is independent of location, and that

all density dependence occurs at the time of settling and depends only on the density of settling juveniles. For the reserve case, we present the details of the analysis for the case in which all adults outside the reserves are caught in the fishery—there is no reproduction outside the reserves. We also describe results for the case of a mixed strategy employing reserves and managed harvests.

We set up simple optimization models describing the yield in each case of interest. There are a number of parameters and functions common to both models. The number of settling juveniles produced per year by each adult is assumed to be m , adults reach maturity at age j , and annual adult survival is a . In the case of reserves, we assume that a fraction c of the coastline is set aside in reserves. We denote the density of adults in year t by n_t . We normalize the length of the coastline we are considering to be 1, so that if the density of organisms is constant over space, then the number (density multiplied by length of coastline) of adult organisms is also n_t .

Although a complete assessment of marine reserves requires an explicit consideration of the potential density dependence (5) in predispersal, larval, and postdispersal components of recruitment, this has not been done to date. Including these features would require a model of such complexity that no

simple conclusions could be drawn. To establish an initial benchmark for reasonably common conditions, we first analyzed a model in which we only allow postdispersal density dependence and only consider the effect of settling juveniles on density dependence. Thus, if the density of larvae attempting to settle is l , then the density successfully reaching the adult, reproductive class (perhaps years later) is $f(l)$. Our results do not depend on the form of density dependence, f .

Traditional fishery models are often phrased in terms of removing a fraction, or a fixed amount, of the available resource each year, producing the same yield in each case. When a fixed fraction H is harvested, the number of adults the following year is the sum of those reaching maturity and those surviving from the previous year multiplied by the probability of escape from harvest

$$n_{t+1} = (1 - H)[f(mn_{t-j}) + an_t] \quad (1)$$

At equilibrium, the population size n satisfies

$$n = (1 - H)[f(mn) + an] \quad (2)$$

The maximum sustainable yield in this model is

$$Y_h = \max\{H[f(mn) + an]\} \quad (3)$$

which is subject to Eq. 2. By solving Eq. 2 for the expression on the right-hand side of Eq. 3, one can rewrite the equation for the maximum sustainable yield for traditional harvesting as

$$Y_h = \max\{[f(mn) + an] - n\} \quad (4)$$

where n is the variable that can be chosen to maximize yield.

In the case of reserves, we assume that the density of organisms in the reserves is n'_r , so the number (not density) of juveniles produced is thus cmn'_r . Because we make the simplifying assumption that the larvae are widely dispersed, we posit that the density of settling juveniles is once again independent of location. Therefore, the density of postdispersal juveniles is equal to cmn'_r , both inside reserves and in the fished areas outside reserves. Thus, inside the reserves, the dynam-

¹Department of Environmental Science and Policy, ²Department of Wildlife, Fish, and Conservation Biology, University of California, Davis, CA 95616, USA.

*To whom correspondence should be addressed. E-mail: amhastings@ucdavis.edu